Supporting Information

of

Highly Stable Iron Carbonyl Complex Delivery Nanosystem for Improving Cancer Therapy

Xiao-Shuang Wang,[†] Jin-Yue Zeng,[†] Min-Jie Li,[†] Qian-Ru Li,[†] Fan Gao,[†] and Xian-Zheng Zhang[†,]*

[†] Key Laboratory of Biomedical Polymers of Ministry of Education, Institute for Advanced Studies (IAS), Department of Chemistry, Wuhan University, Wuhan 430072, P. R. China

* Corresponding author. Email: xz-zhang@whu.edu.cn

Characterization methods

Transmission electron microscopy (TEM) images were captured on a JEM-2100 (JEOL) transmission electron microscope. Scanning electron microscopy (SEM) images were obtained with a Field emission scanning electron microscope (Zesis SIGMA). XPS experiment was performed on an ESCALAB 250Xi X-ray photoelectron spectrometer (Thermo Fisher). The UV-vis absorption spectrum and fluorescence spectrum obtained in the test were collected on a Lambda 35 UV/VIS spectrometer (PerkinElmer) and an LS55 fluorescence spectrometer (PerkinElmer), respectively. Electron paramagnetic resonance spectroscopy of the materials were tested on an FA200 electron paramagnetic resonance spectrometer (JEOL). The size and zeta potential data of the nanoparticles are collected on Nano-ZS ZEN3600 (Malvern Instruments). The cell cytotoxicity was tested by an absorbance microplate reader (SpectraMax 190). *In vivo* fluorescence imaging experiment was performed on a small animal imaging system (IVIS®, Perkin-Elmer). Photothermal imaging is performed with a thermal infrared imaging camera (FLIR Systems AB, Sweden). And, the confocal images were taken on a confocal laser scanning microscope (CLSM, Leica TCS SP8 STED). Photoacoustic imaging experiments were performed on a photoacoustic instrument (VisualSonics Vevo® 2100).

The synthesis of Ag cubes

The synthesis of Ag cube was completed according to the literature with slight modifications.[S1] Briefly, add 90 mL of ethylene glycol to a 250 mL flask and the solution was heated to 150°C for 1 h to remove water. Under argon atmosphere, add 1.2 mL of sodium sulfide ethylene glycol solution (3 mM). Thereafter, 22.5 mL of a PVP ethylene glycol solution (20 mg/mL) was added. After 8-9 min, pipette 7.5 mL of $AgNO_3$ ethylene glycol solution into the flask (48 mg/mL). Wait 15-20 min depending

on the color of the reaction solution. Next, the reaction was quenched by placing the flask in a water bath (10-20°C). After it was cooled to room temperature, the contents were poured into 500 mL of acetone. Centrifuge to obtain the synthesized Ag cubes (9000 g, 20 min).

The preparation of Au nanocages.

650 mL of Ag cube solution was added to the prepared 70 mL of PVP solution (1 mg/mL). The system was heated to a slight boiling at 117°C. After 10 min, the prepared $HAuCl_4$ solution (10 mM) was added dropwise to the Ag cube solution. During the process, the UV absorption peak of the solution was continuously detected until its maximum absorption peak reached between 730-740 nm. After the solution was cooled to room temperature, NaCl was added until the solution was saturated. The etched Au nanocages were collected by centrifugation (11000 rpm, 15-20 min).

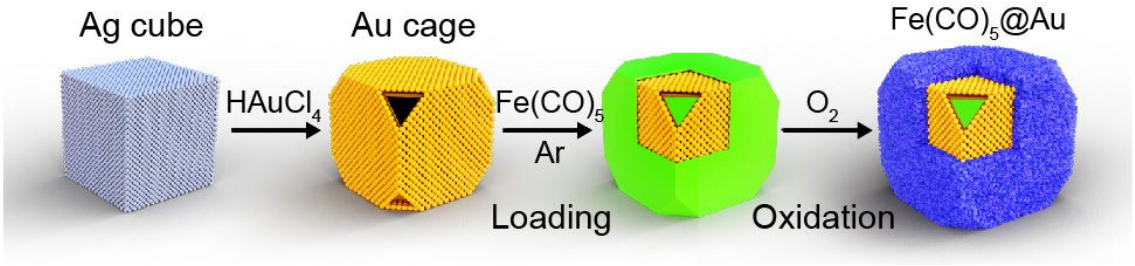

Figure S1 The preparation of $Fe(CO)_5$@Au, including the synthesis of Ag cube and Au cage, loading of $Fe(CO)_5$ and the oxidation process.

The calculation of photothermal conversion efficiency.

We used the methods in the literature to calculate the photothermal conversion efficiency of $Fe(CO)_5$@Au. 1 mL of $Fe(CO)_5$@Au solution (19.2 μg/mL) was applied 808 nm irradiation (1 W/cm^2) until the temperature of the solution reach a platform. Then, the laser was removed and the temperature of the solution was recorded continually. And the photothermal conversion efficiency (η) was calculated *via* the following equations:

$$\eta = \frac{hA(T_{max} - T_{amb}) - Q_s}{I\left(1 - 10^{-A_\lambda}\right)}$$

Where T_{max} is the maximum temperature on the heating curve and Tamb is the ambient temperature of the surroundings. Qs was measured independently to be Qs = (5.4 * 10^{-4}) I J*s-^{1}. I refers to the input power. And A_λ is the absorbance of the solution at wavelength λ.

In order to get the hA, θ, a dimensionless driving force temperature, is introduced.

$\theta = \frac{T_{amb} - T}{T_{amb} - T_{max}}$And a sample system time constant τ_s

$$\tau_s \equiv \frac{\sum_i m_i C_{p,i}}{hA}$$

m is the mass and C is the heat capacity.

When laser irradiation ceases, we can get an equation about τ and θ:

$$\frac{d\theta}{dt} = \frac{-\theta}{\tau_s}$$

Take the point on the cooling period curve and make time *vs* -lnθ graph, the slope obtained by linear fitting is τ_s.[S2] According to **Figure** S12 and S13, τ_s in this work is determined to be -188.11. Then, the relevant test and calculation data were substituted

into the above formula, and the photothermal conversion efficiency of $Fe(CO)_5$@Au can be obtained, ~ 54.02%.

Section S2 Cytotoxicity and cell staining experiments

Cell culture

4T1 cells were cultured in RPMI Medium 1640 with 10% fetal calf serum (FBS) and 1% antibiotics (penicillin-streptomycin, 10 000 U/mL) at 37°C in a humidified atmosphere containing 5% CO_2.

Cytotoxicity assay

The cytotoxicity against 4T1 cells was measured *via* MTT assay. The cells were cultured in a 96-well plate and incubated for 24 h at 37°C. Thereafter, gradient concentrations of $Fe(CO)_5$@Au nanocages were added into each well. After incubation for another 4 h, the cells were irradiated with an 808 nm laser (1.5 W/cm^2) for 150 s. As for the control groups, 4T1 cells and $Fe(CO)_5$@Au were co-cultured for 4 h without 808 nm irradiation. Afterward, the cells were cultured for 24 h and 20 μL of MTT (5 mg/mL in PBS) was added and incubated for another 4 h. After that, the supernatant was removed and 150 μL of dimethyl sulfoxide (DMSO) was added. After shaking for several min, the optical density (OD) at 570 nm was recorded by a microplate reader model 550. The cell viability (%) was calculated according to the following formula: cell viability (%) = OD (sample) × 100/OD (control), where OD (control) and OD (samples) represent the absorbance at 570 nm in the absence and presence of $Fe(CO)_5$@Au nanocages, respectively.

Detection of intracellular CO production.

A certain number of 4T1 cells were evenly seeded into 1 ml glass dishes, and cultured in an incubator for 24 h. After discarding the supernatant, the $Fe(CO)_5$@Au nanocage medium solution (30 μg/mL) was added to the glass dish. After 4 h, it was irradiated

with a laser at 808 nm (1 W/cm^2, 3 min). CO probe was added to co-culture with cells half an hour before light exposure. The fluorescence of the sample was detected using CLSM.

Reactive oxygen species (ROS) detection.

The intracellular ROS was measured using DCFH-DA as the indicator. Briefly, after treating 4T1 cells with $Fe(CO)_5$@Au (30 μg/mL) for 6 h, change the previous medium to the well-prepared DCFH-DA staining solution (1×10^{-6} M). The cells were incubated for another 30 min. Then, the cells were irradiated (808 nm, 1 W/cm^2) for 3 min. All of the cells were observed by CLSM with a laser at 488 nm.

JC-1 staining.

The 4T1 cells were seeded into 1 ml glass dishes and cultured in a cell incubator for 24 h. The $Fe(CO)_5$@Au nanocages were diluted with the cell culture medium to appropriate concentration and added to the dish. After 4 h of incubation, an 808 nm laser was used to irradiate the cells for 3 min (1 W/cm^2). After that, the supernatant was discarded and a pre-prepared JC-1 staining solution (10 μg/mL) was added. The cells were placed in the incubator and stained for 30 min. Finally, the cells were washed thoroughly with PBS and the fluorescence was measured by confocal laser scanning microscope (CLSM, Leica TCS SP8 STED).

Section S3 Animal imaging in vivo

Fluorescence imaging. 4T1 tumor model was established by injecting 4T1 cells (1×10^6) subcutaneously on the left back of the BALB/c mice (5-6 weeks old). Once the tumor volume reached 100 mm^3 around, 4T1 tumor bearing mice were intravenously injected with $Fe(CO)_5$@Au nanocages which were marked with HS-PEG2000-Cy5 for imaging studies. At the scheduled time after injection, the tumor imaging was carried out *via* a living image IVIS® spectrum (Perkin-Elmer).

Photothermal imaging. The tumor-bearing mouse model was the same as that used for fluorescence imaging. $Fe(CO)_5$@Au nanocages (1 mg/mL, 120 μL) were injected into the mouse by intravenous injection. After 6 h, photothermal imaging of mice is performed with a thermal infrared imaging camera (FLIR Systems AB, Sweden).

Photoacoustic imaging. The tumor-bearing mouse model was also the same as that used for fluorescence imaging. Mice were injected $Fe(CO)_5$@Au nanocages (1 mg/mL, 120 μL) by intravenous injection. Photoacoustic imaging was performed on mice at different time points (0 h, 2 h, 6 h, 10 h, 24 h). And, the imaging data was collected by a photoacoustic instrument (VisualSonics Vevo® 2100).

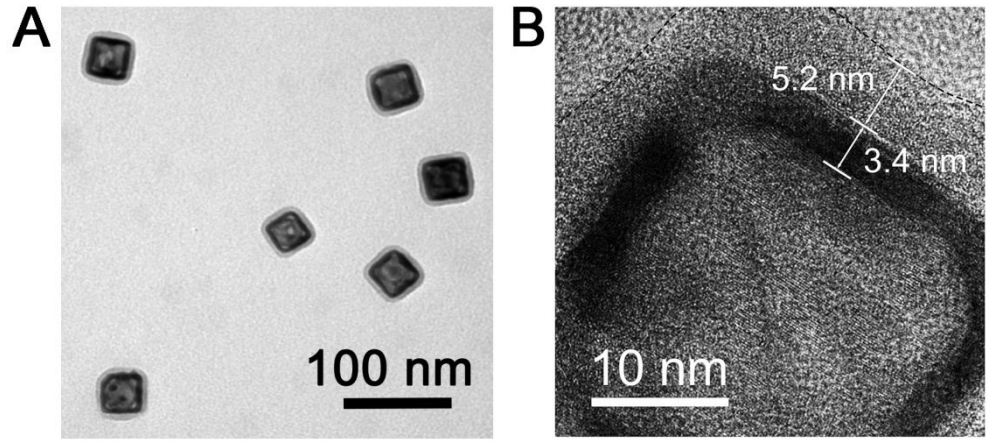

Figure S2 (A) TEM image and (B) high-resolution TEM image of $Fe(CO)_5$@Au.

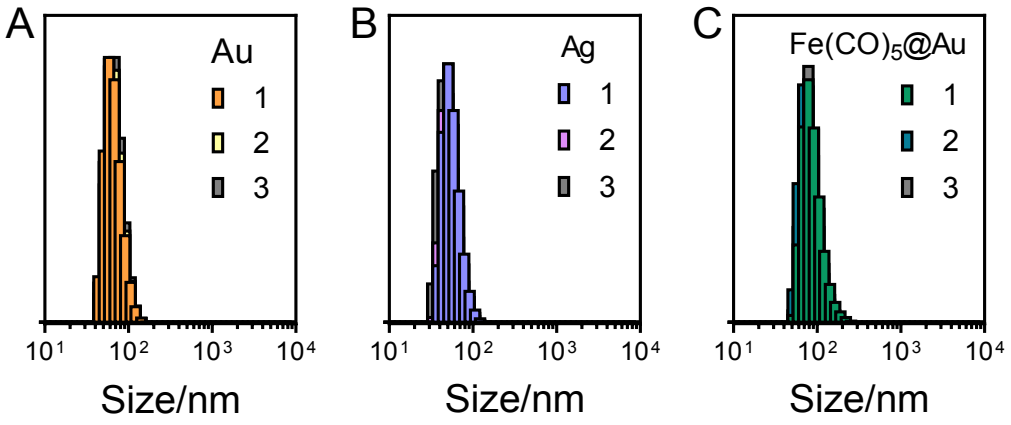

Figure S3 DLS analysis of (A) Ag cube, (B) Au nanocage and (C) $Fe(CO)_5$@Au nanoparticles.

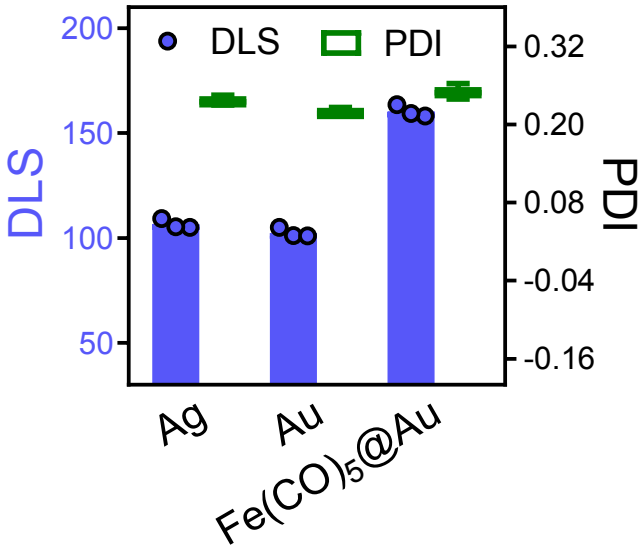

Figure S4 DLS and the corresponding polymer dispersity index (PDI) of Ag cube, Au nanocage and $Fe(CO)_5$@Au.

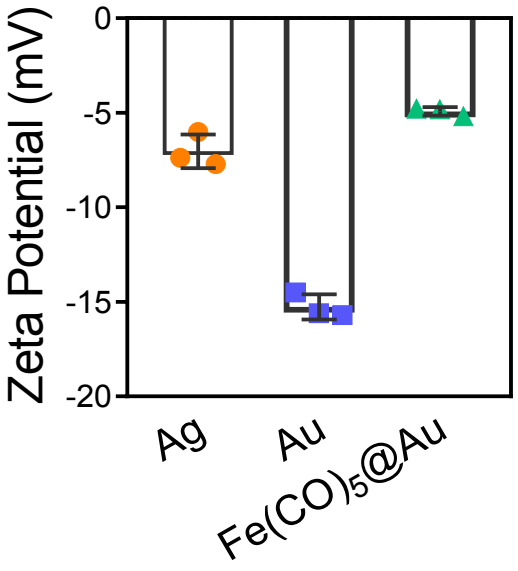

Figure S5 Zeta potential of Ag cube, Au nanocage and $Fe(CO)_5$@Au.

In order to detect the composition and elemental valence of $Fe(CO)_5$@Au, XPS experiment was performed on an ESCALAB 250Xi X-ray photoelectron spectrometer (Thermo Fisher).

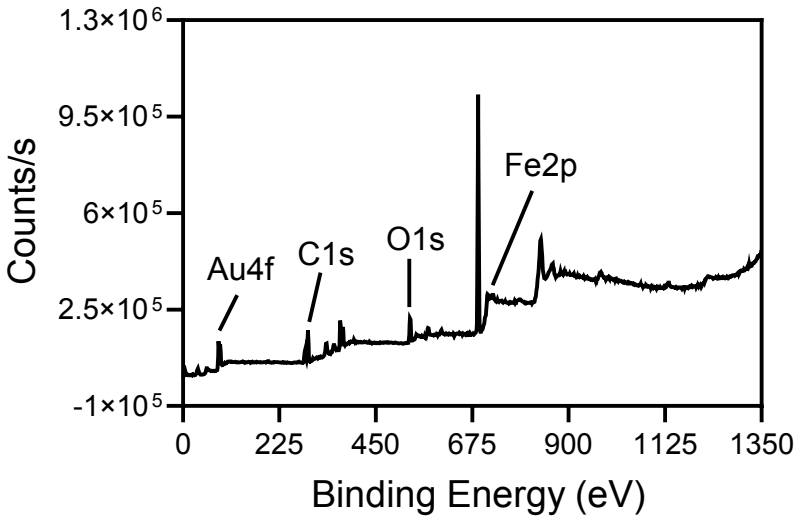

Figure S6 XPS spectrum of $Fe(CO)_5$@Au.

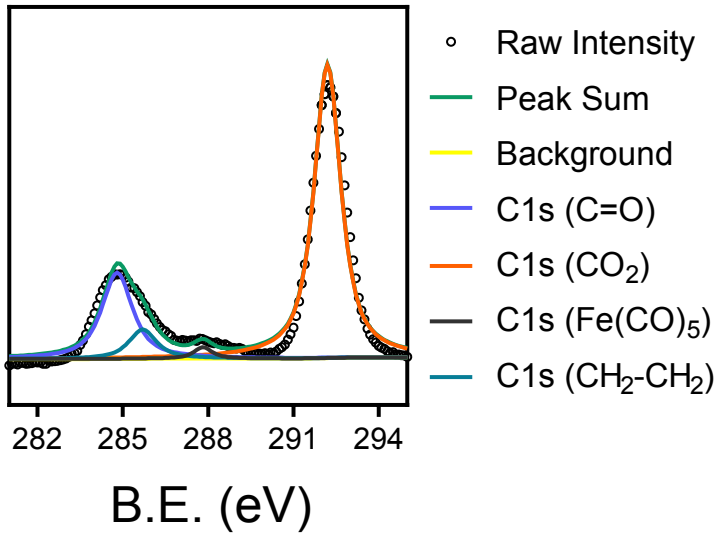

Figure S7 XPS spectra of C in $Fe(CO)_5$@Au.

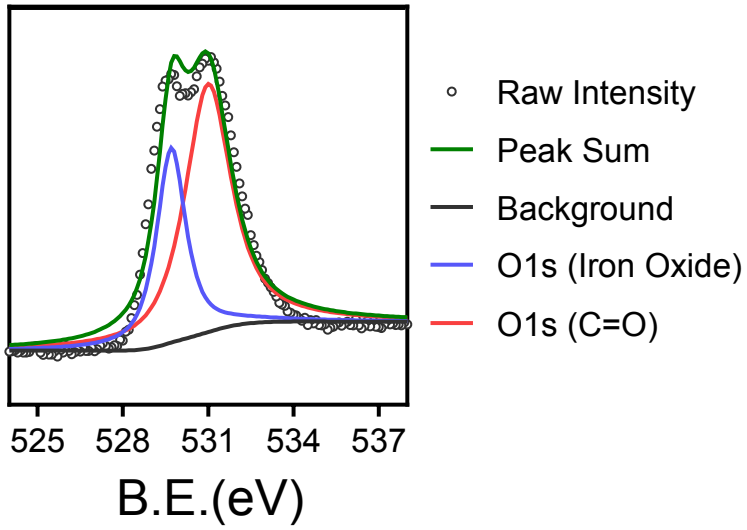

Figure S8 XPS spectra of O in $Fe(CO)_5$@Au.

To further investigate the loading of $Fe(CO)_5$ and the formation of iron oxide shell, the loading processes were performed under Ar and O_2, respectively.

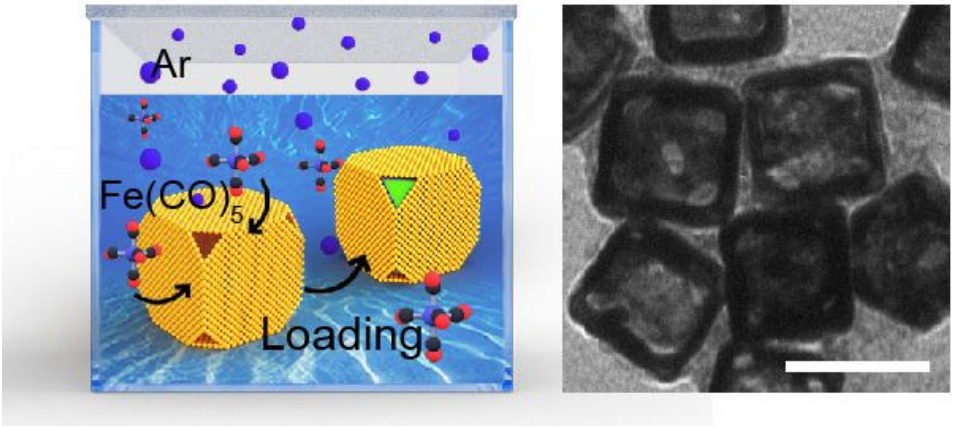

Figure S9 The loading process $Fe(CO)_5$ into Au nanocage under Ar and the corresponding TEM image of $Fe(CO)_5$@Au (scale bar, 50 nm).

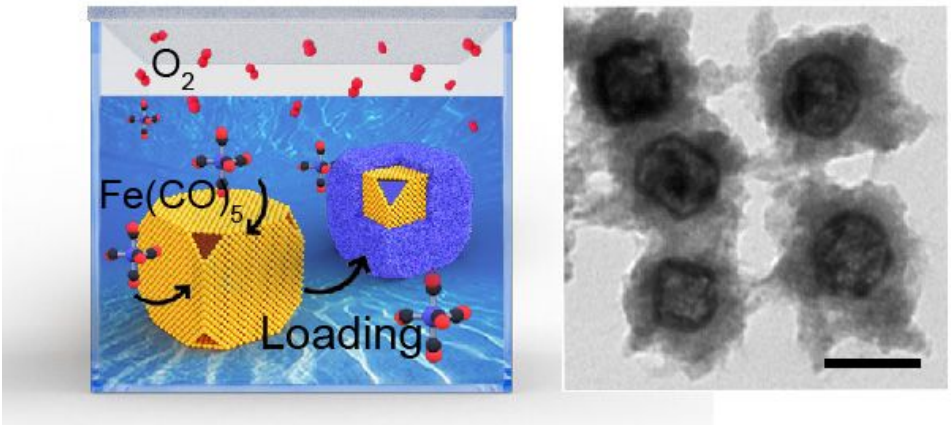

Figure S10 The loading process $Fe(CO)_5$ into Au nanocage under O_2 and the corresponding TEM image of $Fe(CO)_5$@Au (scale bar, 50 nm).

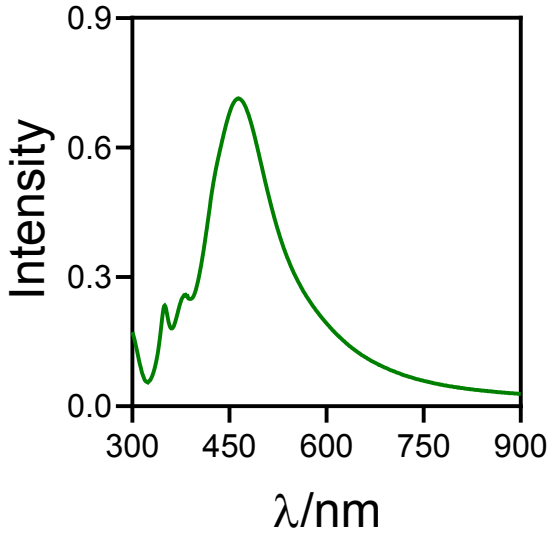

Figure S11 UV-vis spectrum of Ag cube.

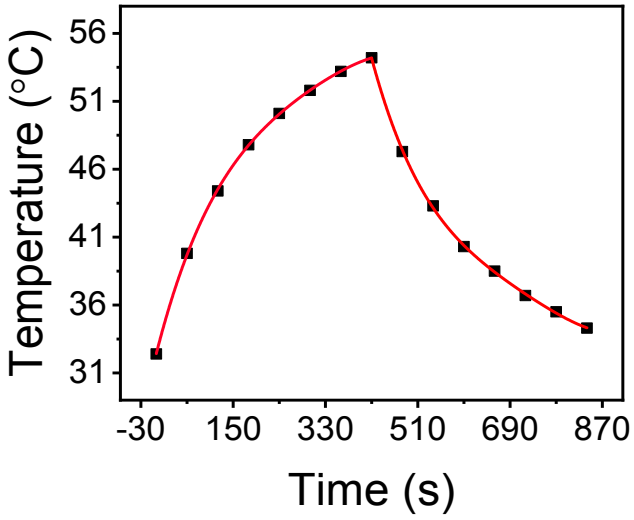

Figure S12 Heating/Cooling experiment of 19.2 μg/mL $Fe(CO)_5$@Au under 1 W/cm^2 808 nm irradiation.

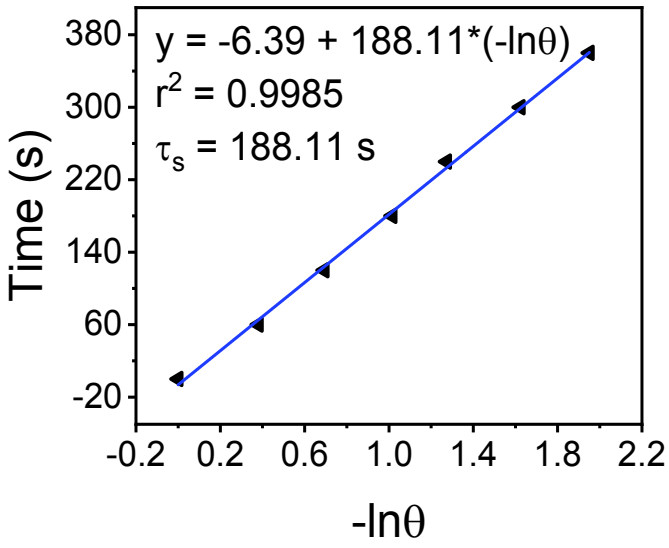

Figure S13 Time from the cooling period *versus* –ln θ (θ = ΔT / ΔT_{max}, ΔT and ΔT_{max} represent the maximun and the real time temperature changes, respectively) and the time constant for heat transfer is determined to be τs = 188.11 s.

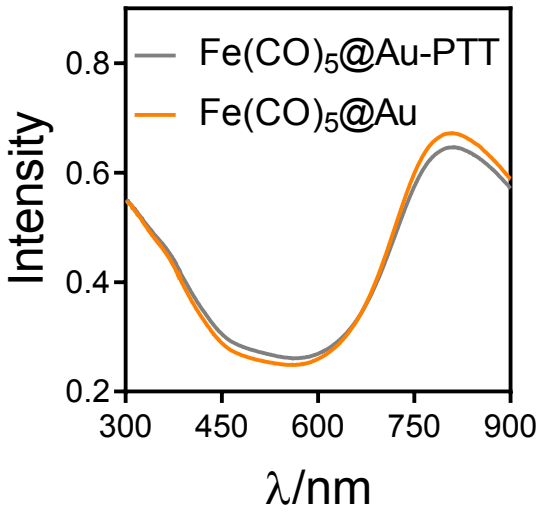

Figre S14 UV-vis spectra of $Fe(CO)_5$@Au before and after the 808 nm irradiation.

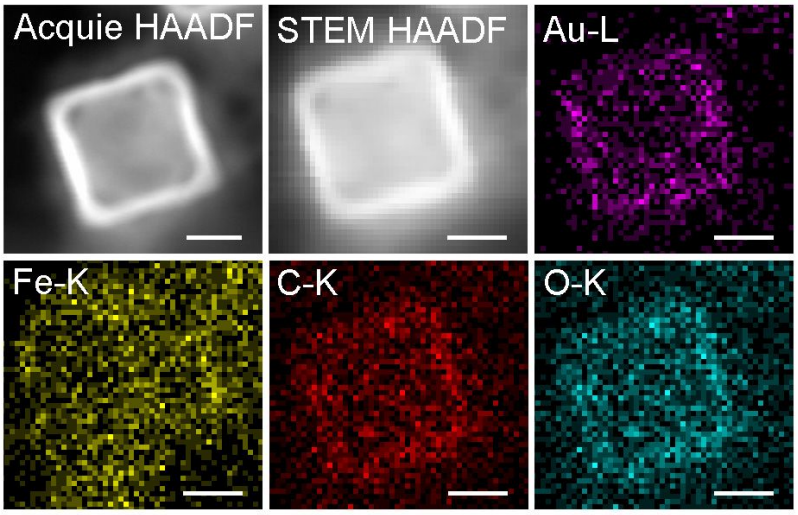

Figure S15 TEM-EDS elemental mapping images of $Fe(CO)_5$@Au before and after the 808 nm irradiation (scale bar, 20 nm).

Detection of extracellular CO production. CO detection solution was prepared in advance according to literature methods.[S3] The test samples (40 μg/mL of $Fe(CO)_5$@Au nanocage, 40 μg/mL of Au nanocage and H_2O) and the detection solution were mixed uniformly. The fluorescence intensity at 514 nm of the sample solution under different irradiation time was tested.

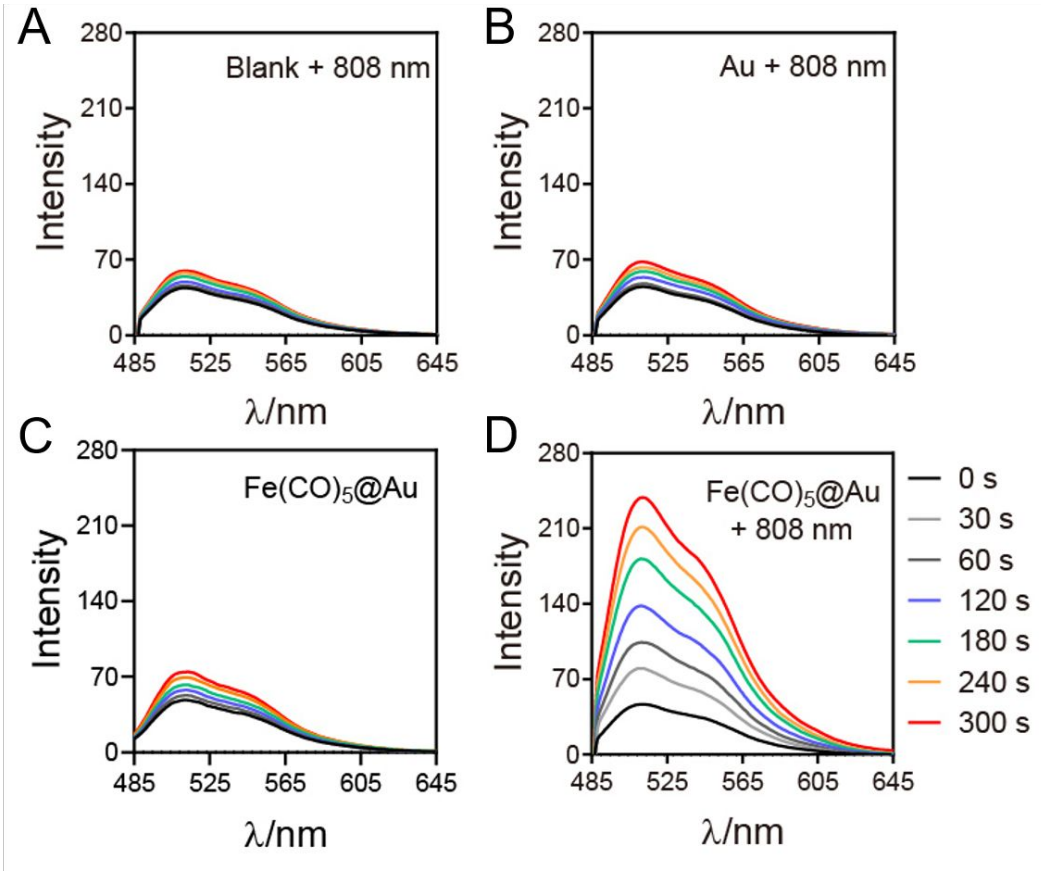

Figure S16 Fluorescence spectrum changes of CO probe with (A) blank + 808 nm irradiation, (B) Au + 808 nm irradiation, (C) $Fe(CO)_5$@Au and (D) $Fe(CO)_5$@Au + 808 nm irradiation.

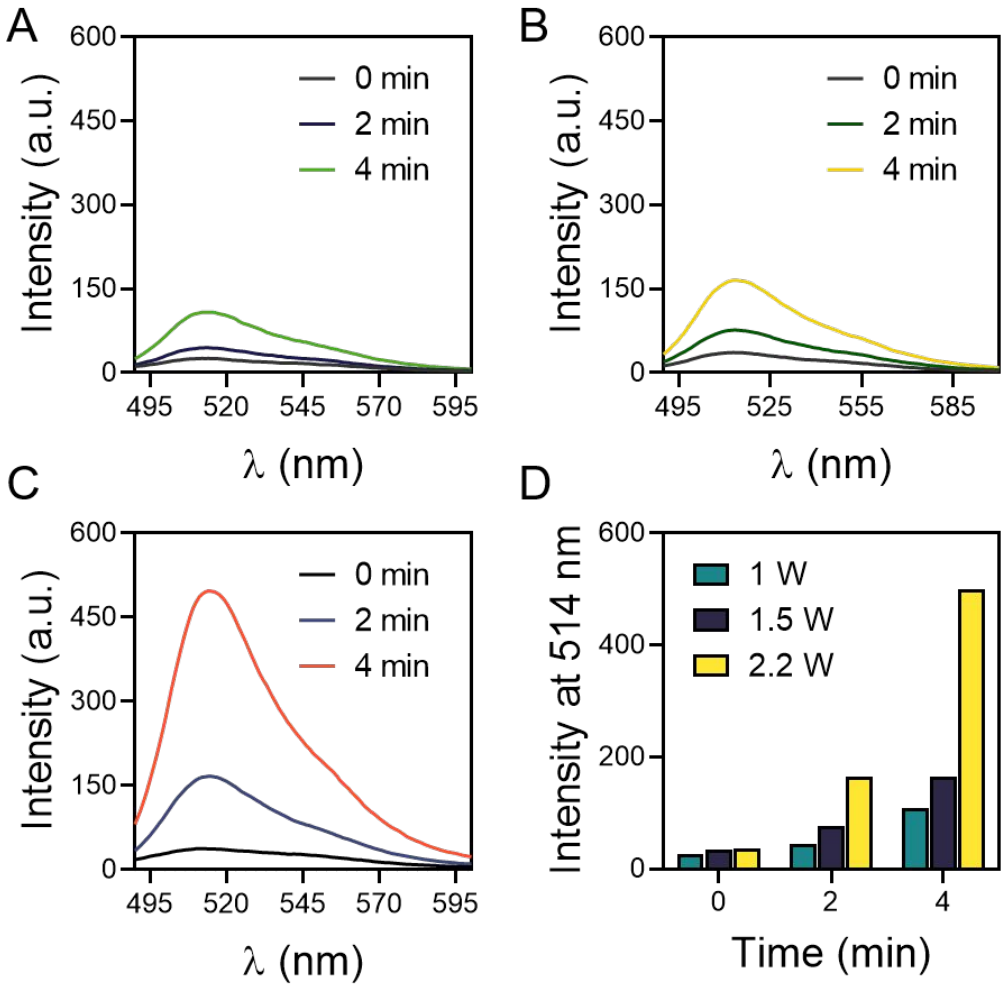

Figure S17 Fluorescence spectrum changes of the CO probe with $Fe(CO)_5$@Au under different laser power input: (A) 1 W, (B) 1.5 W, (C) 2.2 W and (D) their quantification.

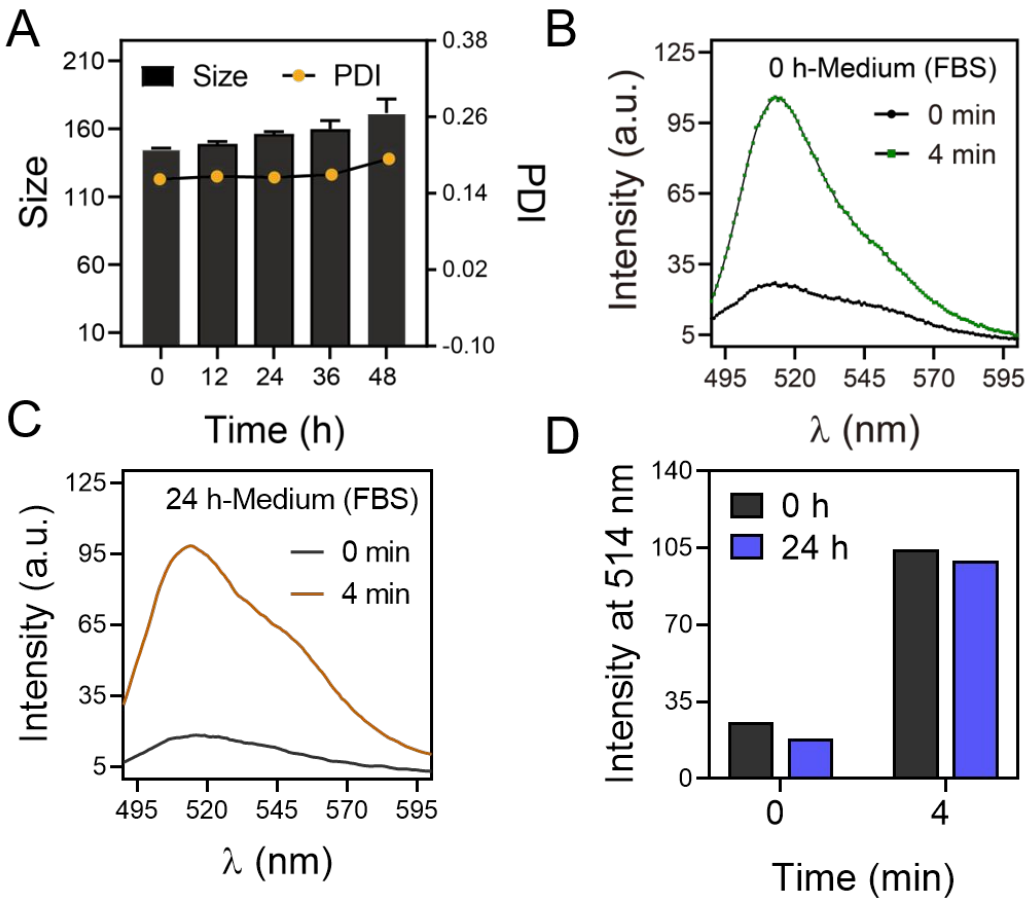

Figure S18 (A) The size and PDI of $Fe(CO)_5$@Au after treated with culture medium containing fetal bovine serum (FBS) for 0 h, 24 h and 48 h. Fluorescence spectrum changes of the CO probe with $Fe(CO)_5$@Au in culture medium containing FBS for (B) 0 h and (C) 24 h as well as (D) their quantification at 514 nm.

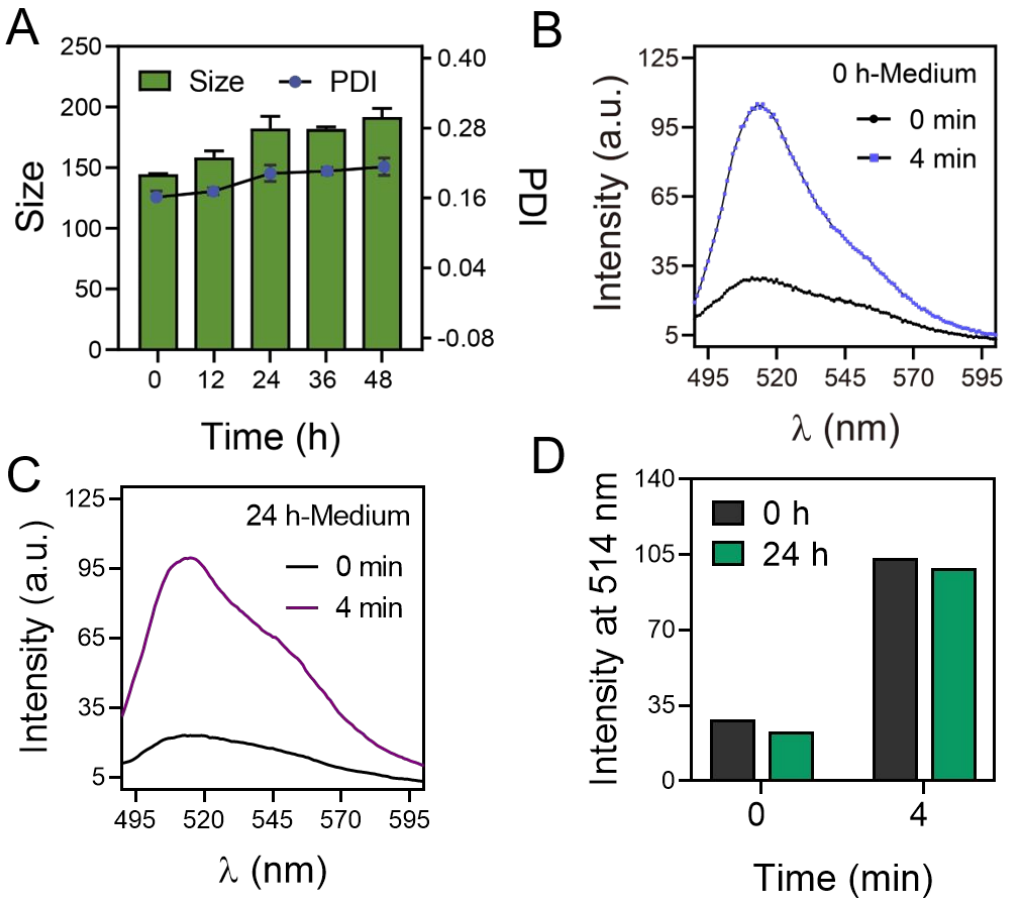

Figure S19 (A) The size and PDI of $Fe(CO)_5$@Au after treated with pure culture medium for 0 h, 12 h, 24 h 36 h and 48 h. Fluorescence spectrum changes of the CO probe with $Fe(CO)_5$@Au in pure culture medium for (B) 0 h and (C) 24 h as well as (D) their quantification at 514 nm.

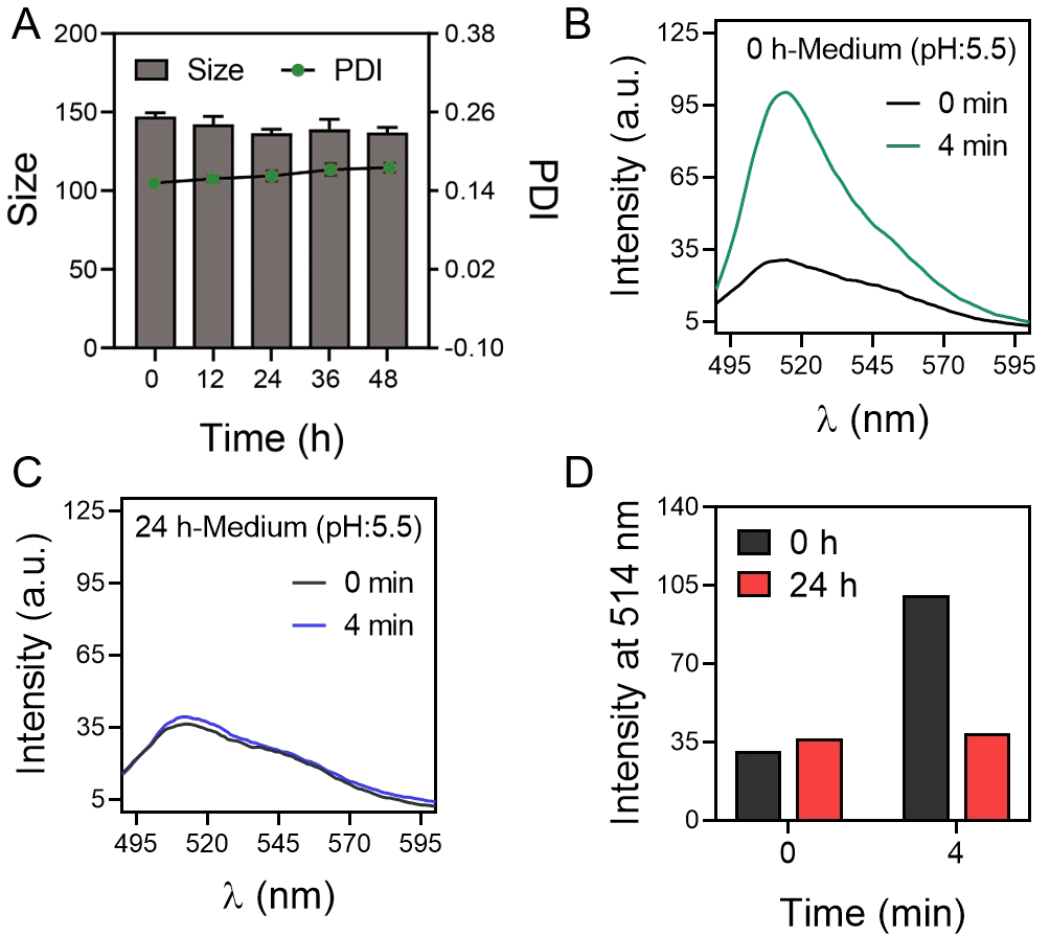

Figure S20 (A) The size and PDI of $Fe(CO)_5$@Au after treated with acidic culture medium (pH=5.5) for 0 h, 24 h and 48 h. Fluorescence spectrum changes of the CO probe with $Fe(CO)_5$@Au in acidic culture medium (pH=5.5) for (B) 0 h and (C) 24 h as well as (D) their quantification at 514 nm.

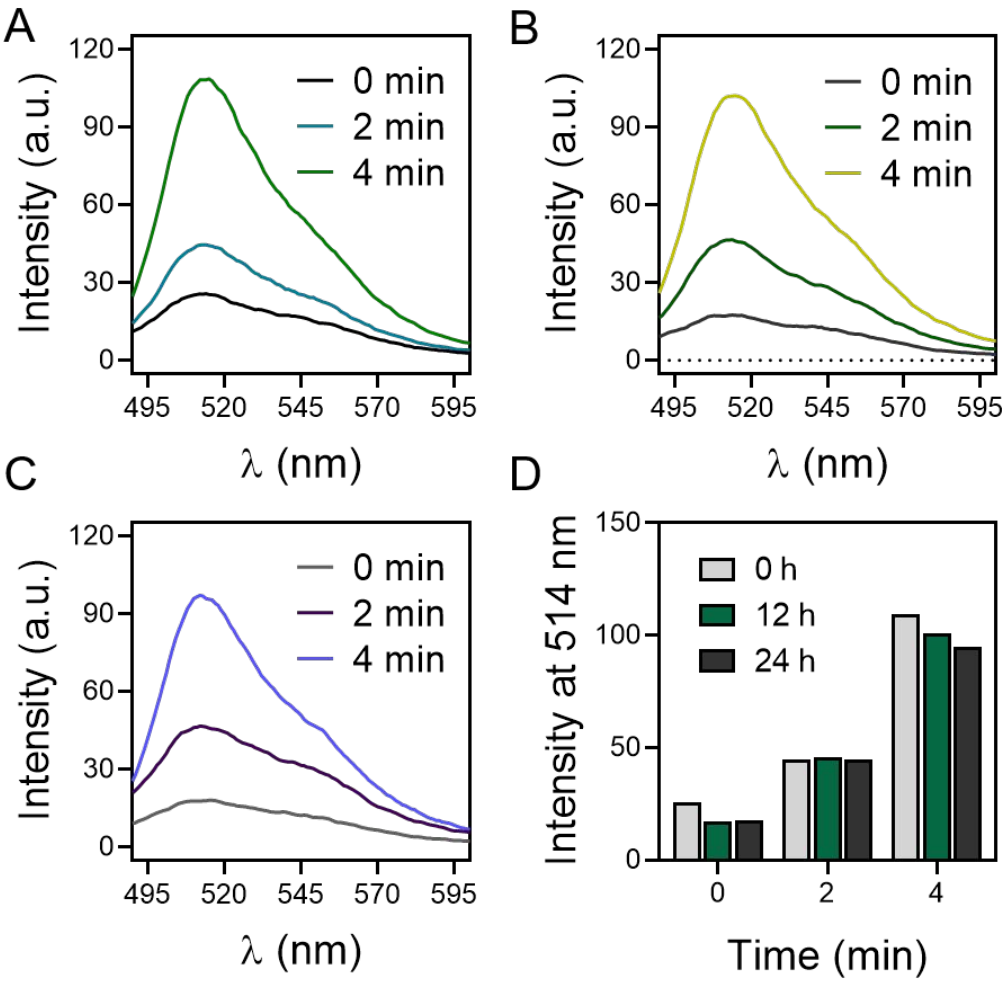

Figure S21 Fluorescence spectrum changes of the CO probe with $Fe(CO)_5$@Au after being aged for (A) 0 h, (B) 12 h and (C) 24 h under aerobic conditions and (D) their quantification at 514 nm.

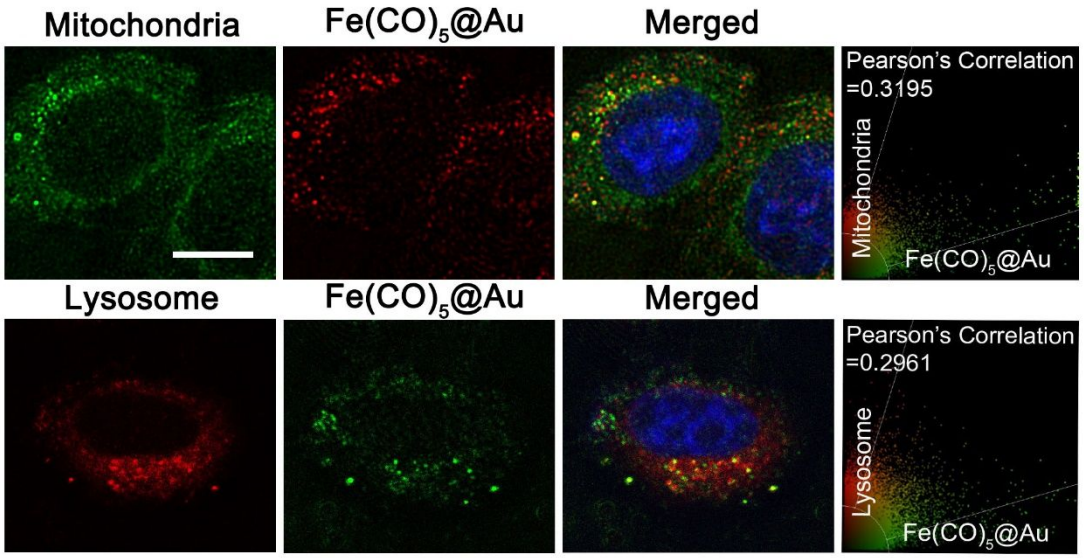

Figure S22 Colocalization analysis of $Fe(CO)_5$@Au with mitochondria and lysosomes (scale bar, 10 μm).

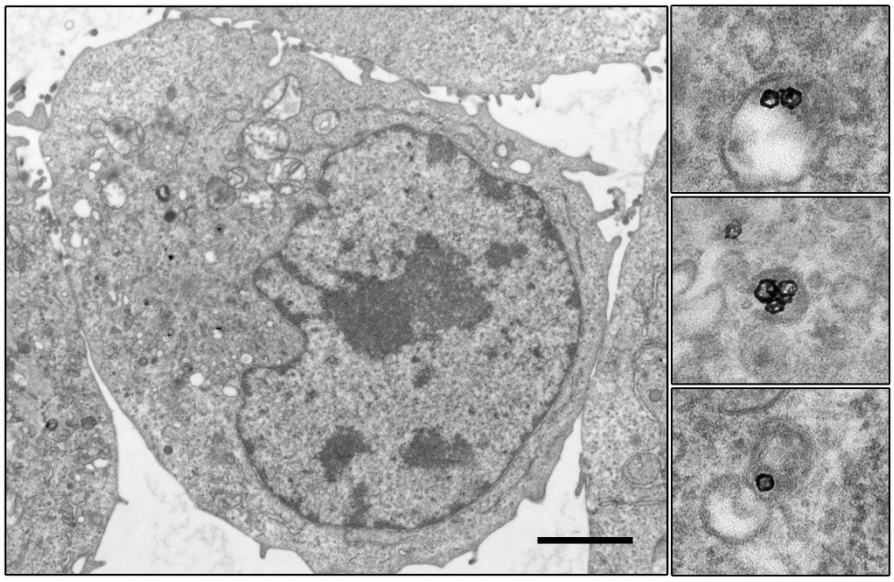

Figure S23 Bio-electron micrograph of 4T1 cells co-cultured with $Fe(CO)_5$@Au for 6 h (scale bar, 2μm).

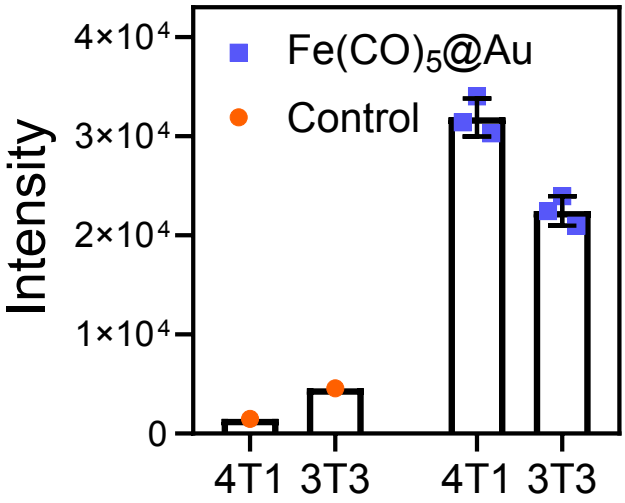

Figure S24 Quantitative analysis of $Fe(CO)_5$@Au endocytosis by 3T3 cells and 4T1 cells.

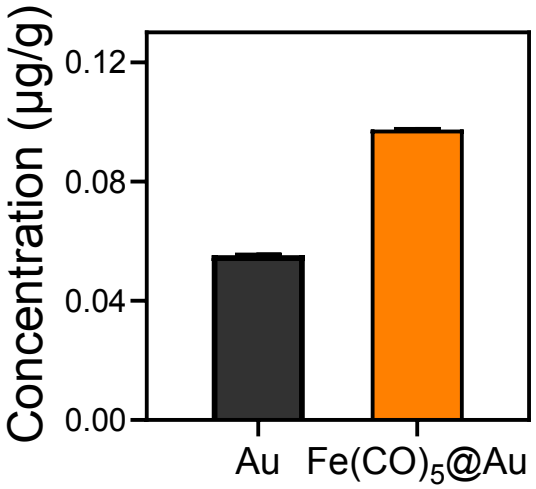

Figure S25 Quantification of Au endocytosed into the 4T1 cells treated with Au and $Fe(CO)_5$@Au.

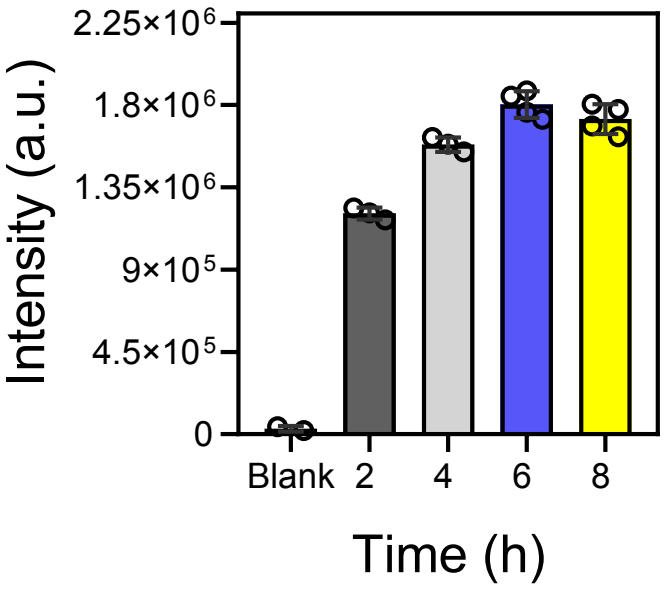

Figure S26 The amount of $Fe(CO)_5$@Au endocytosed by the 4T1 cells after co-cultured for different time.

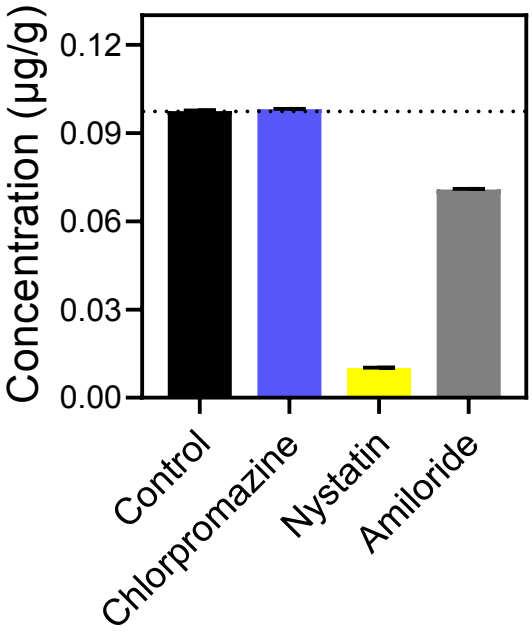

Figure S27 The amount of Au endocytosed by 4T1 cells treated with chlorpromazine (10 μg/mL), nystatin (30 μg/mL) and amiloride (15 μg/mL).

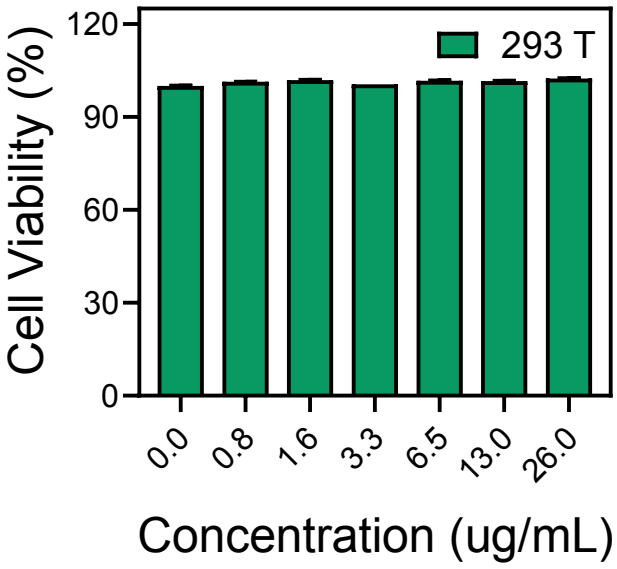

Figure S28 Cytotoxicity of $Fe(CO)_5$@Au against normal cells (293 T).

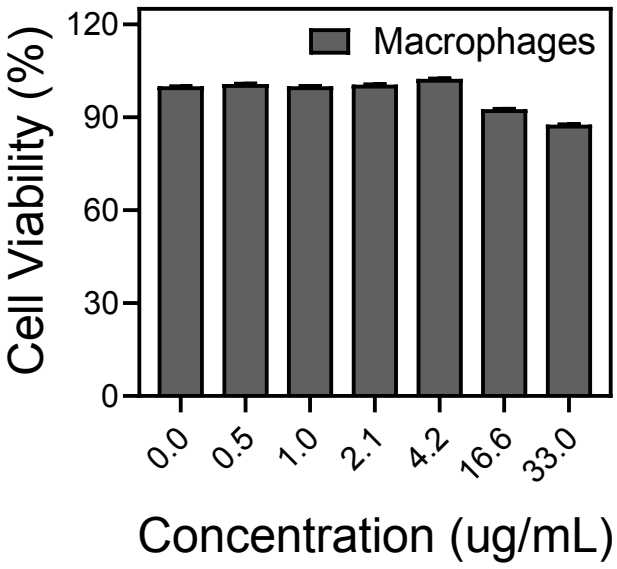

Figure S29 Cytotoxicity of $Fe(CO)_5$@Au against macrophages.

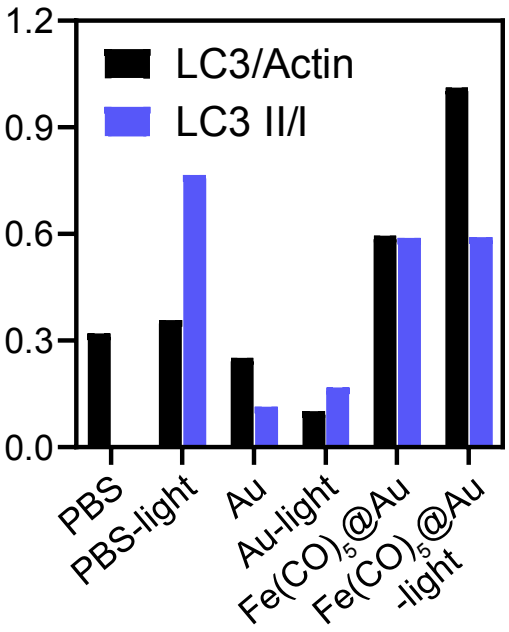

Figure S30 Quantitative analysis results of WB for LC3 protein.

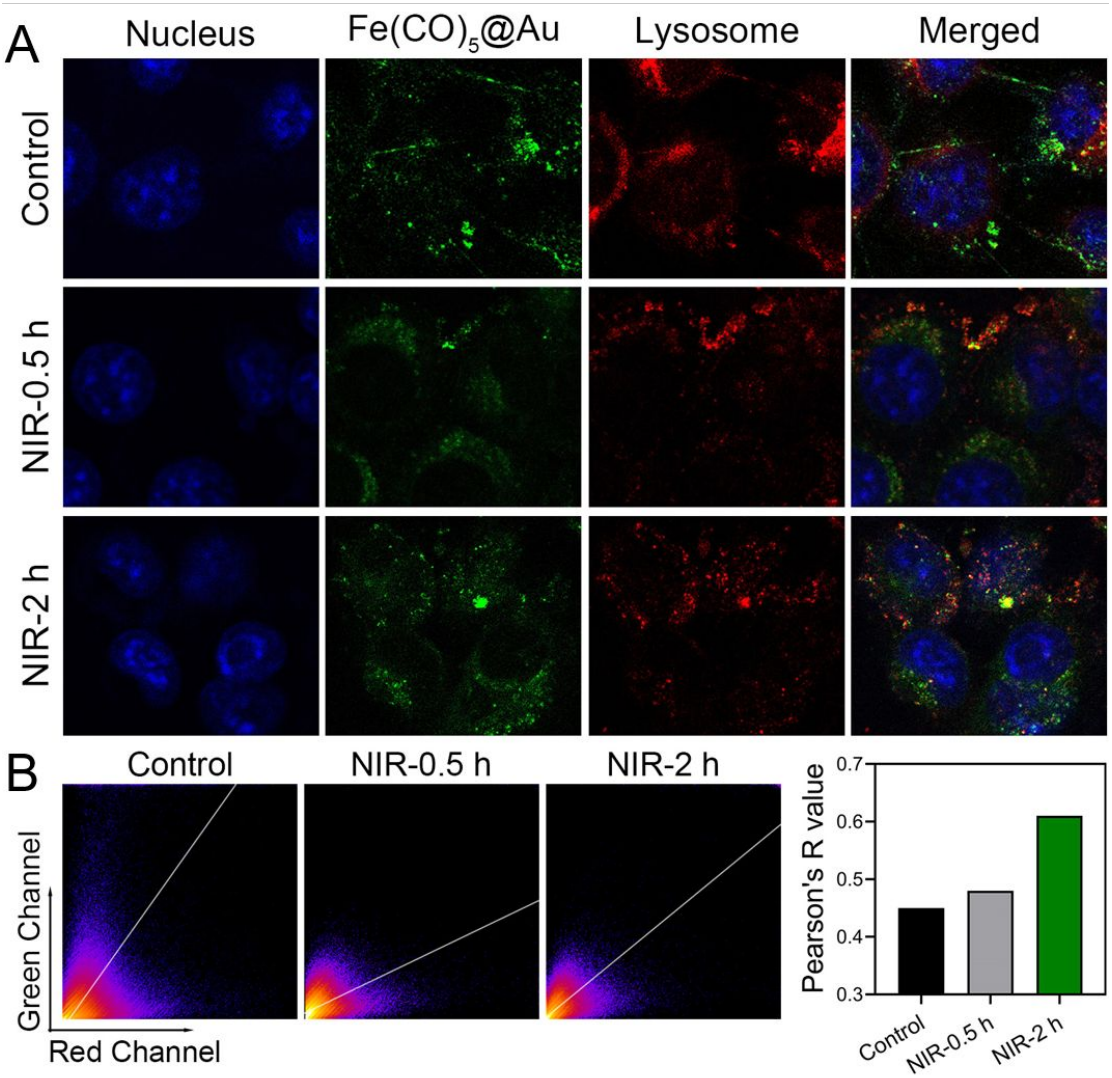

Figure S31 (A) Colocalization images of $Fe(CO)_5$@Au (cy5) and lysosomes without irradiation, 0.5 h after irradiation and 2 h after irradiation. (B) Corresponding co-location analysis results.

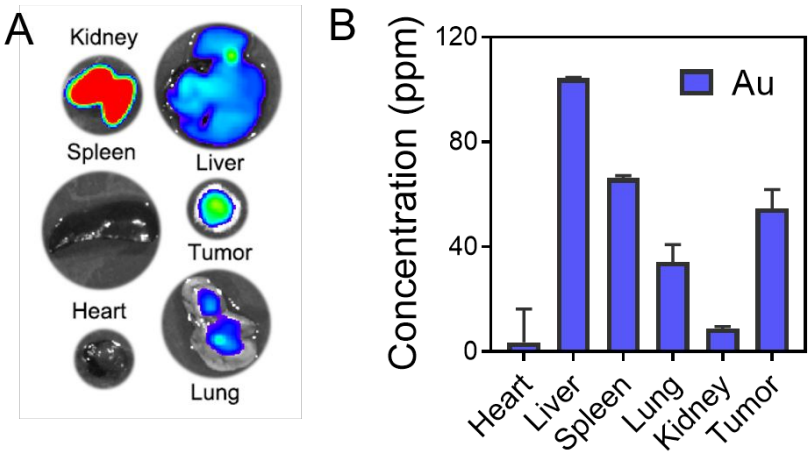

Figure S32 (A) *Ex vivo* fluorescence imaging of $Fe(CO)_5$@Au (HS-PEG-Cy5) in the spleen, liver, heart, tumor, kidney and lung (8 h after injection). (B) Corresponding Au content in main organs and tumor *via* ICP-MS.

Absorption of light in the near-infrared region makes $Fe(CO)_5$@Au great photoacoustic imaging capabilities. We tested the photoacoustic imaging effect of $Fe(CO)_5$@Au with a photoacoustic instrument (VisualSonics Vevo® 2100).

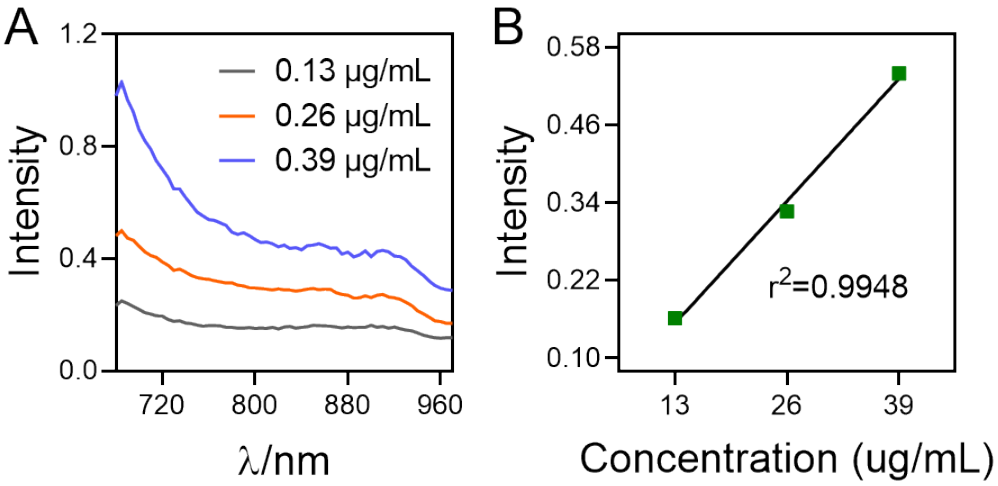

Figure S33 (A) PA signal curves of $Fe(CO)_5$@Au with different concentrations. (B) Calibration curve of PA signal *versus* $Fe(CO)_5$@Au concentration.

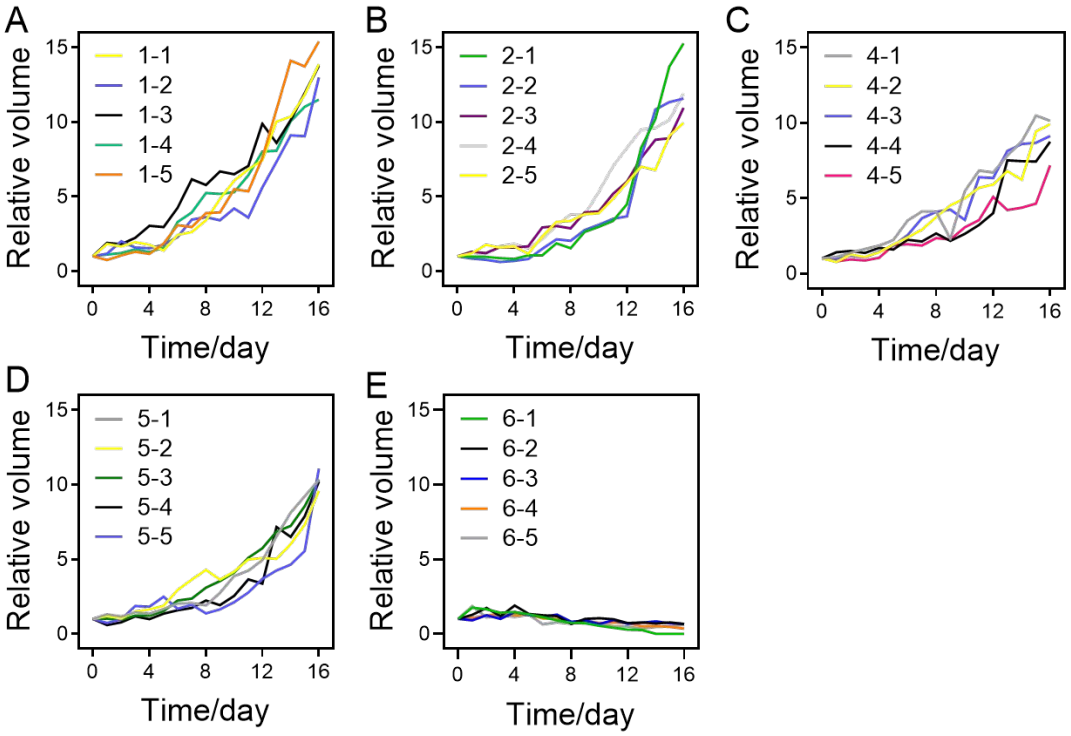

Figure S34 Tumor volume curves of mice after treated with (A) PBS, (B) PBS-light, (C) Au-light, (D) $Fe(CO)_5$@Au and (E) $Fe(CO)_5$@Au-light.

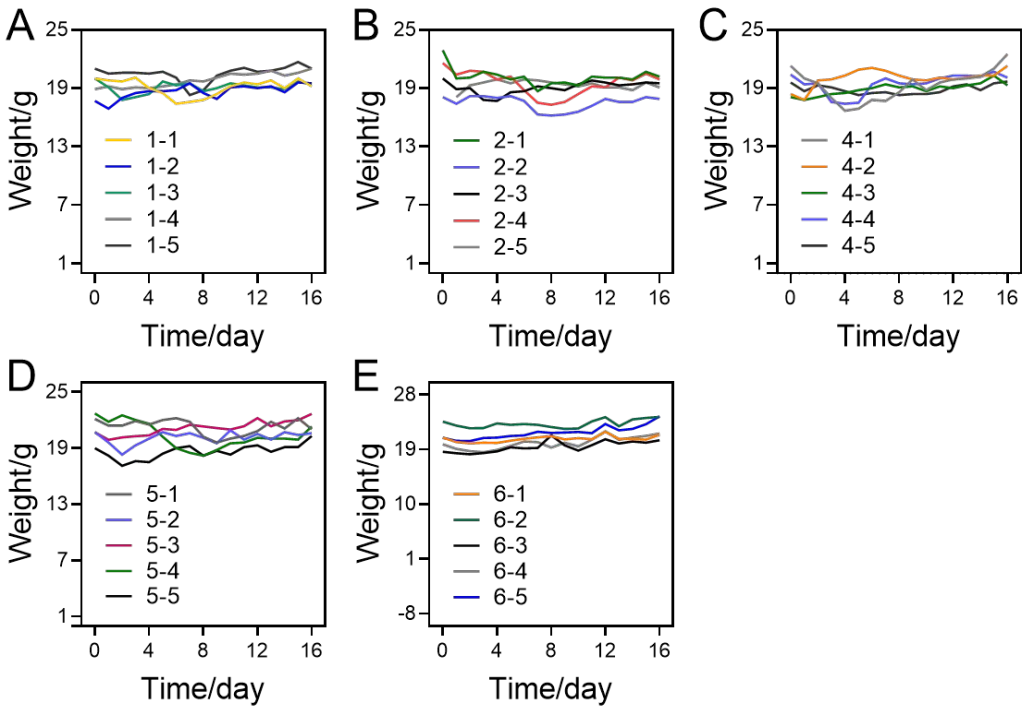

Figure S35 Body weight changes of mice after treated with (A) PBS, (B) PBS-light, (C) Au-light, (D) $Fe(CO)_5$@Au and (E) $Fe(CO)_5$@Au-light.

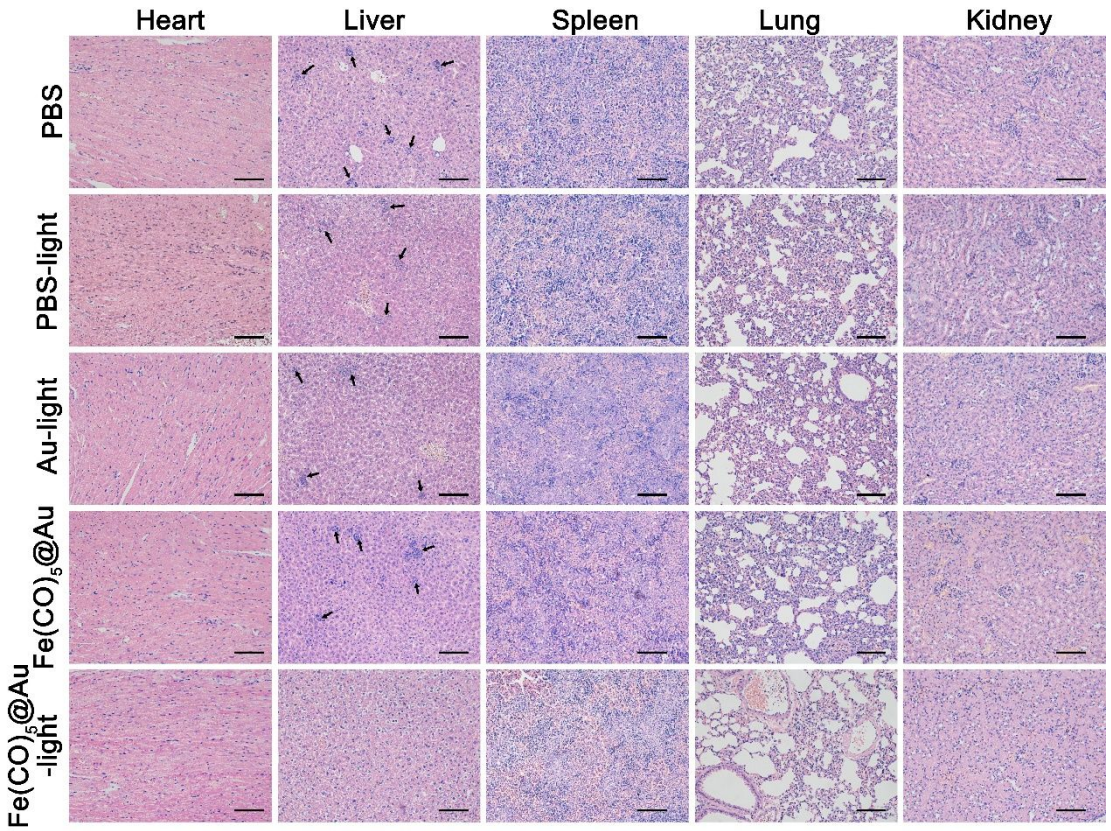

Figure S36 H&E staining of the organs after treatment (scale bar, 100 μm). The black arrows refer to the metastasis.

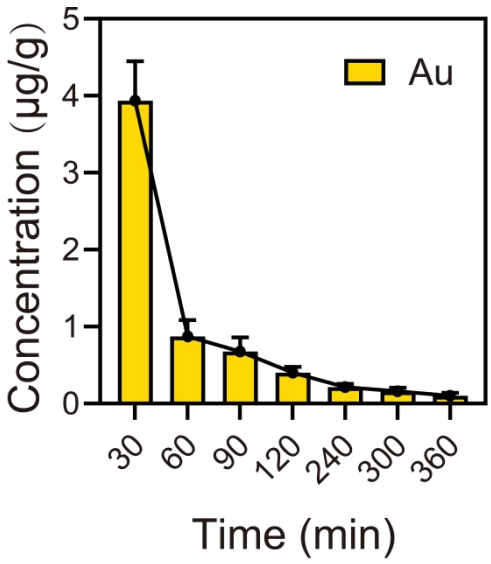

Figure S37 The pharmacokinetics of $Fe(CO)_5$@Au in the blood.

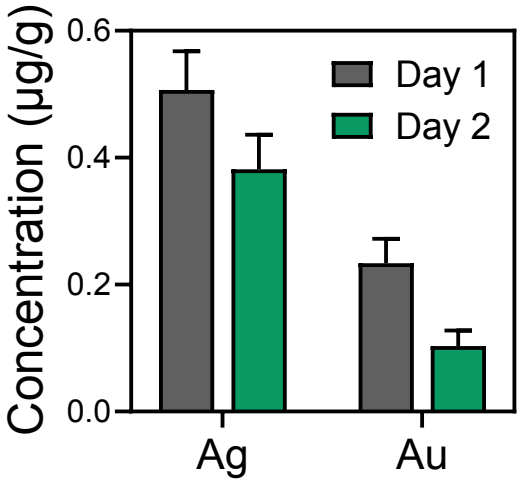

Figure S38 The amount of Ag and Au in the excrement of mice injected with $Fe(CO)_5$@Au on the 1st day and 2nd day.

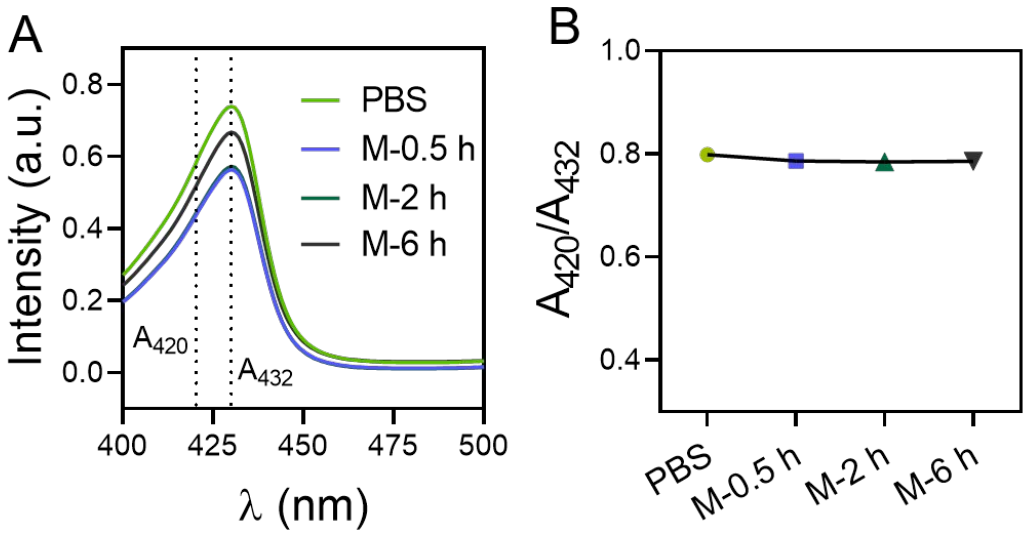

Figure S39 (A) UV-vis spectra of blood of normal mouse and mice after the injection of $Fe(CO)_5$@Au for 0.5 h, 2 h and 6 h. (B) A_{420}/A_{432} of the UV-vis spectrum to determine the content of COHb.

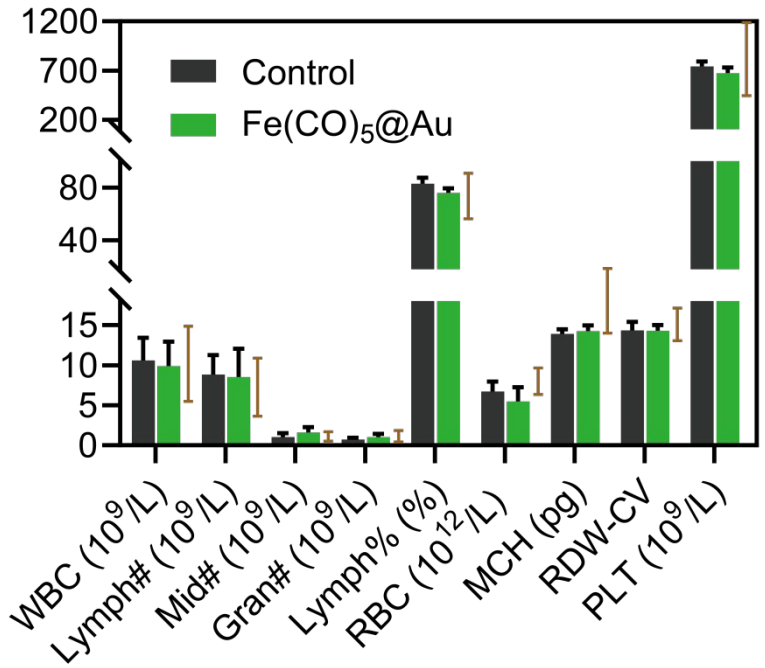

Figure S40 The blood routine examination 1 h post injection of $Fe(CO)_5$@Au and control. The brown bars refer to the reference range.

References

S1. Skrabalak, S. E.; Au, L.; Li, X.; Xia, Y. Facile Synthesis of Ag Nanocubes and Au Nanocages. *Nat. Protoc.* **2007,** *2,* 2182-2190.

S2. Roper D K.; Ahn W.; Hoepfner M. Microscale Heat Transfer Transduced by Surface Plasmon Resonant Gold Nanoparticles. *J. Phys. Chem. C* **2007,** *111,* 3636-3641.

S3. Feng, S.; Liu, D.; Feng, W.; Feng, G. Allyl Fluorescein Ethers as Promising Fluorescent Probes for Carbon Monoxide Imaging in Living Cells. *Anal. Chem.* **2017,** *89,* 3754-3760.